Technische Universität Ilmenau
Institut für Mathematik

Preprint No. M **13/03**

A continuum model of passive vibrissae

Joachim Steigenberger

März 2013

Impressum:
Hrsg.: Leiter des Instituts für Mathematik
Weimarer Straße 25
98693 Ilmenau
Tel.: +49 3677 69-3621
Fax: +49 3677 69-3270
http://www.tu-ilmenau.de/math/

ilmedia

A Continuum Model of Passive Vibrissae

Joachim Steigenberger

March 8, 2013

Abstract

A passive vibrissa (whisker) is modeled as an elastic bending rod that interacts with a rigid obstacle in the plane. Aim is to see details of what happens in quasistatically scanning the obstacle. To this end the differential equations emerging from Bernoulli's rod theory are solved by elliptic integrals followed by numerical evaluation. As a supplement we consider the analogous scanning problem using a simple rigid body model for the vibrissa.

Keywords: Biomechanics, vibrissae, mechanical sensing
MSC: 92C10, 74L15, 74K10

1 Introduction

Most mammals like mice, cats, and seals are equipped with *vibrissae*. These are special tactile sensor organs which contribute to the perception of the environment by noticing environmental vibrations or contact with an external obstacle. A vibrissa is hair-like and it is subcutaneously anchored in the so-called follicle-sine-complex. The latter contains mechano-receptors and a chamber filled with blood of controllable pressure, and it is surrounded by various muscles. Thereby both stiffness and viscosity of the anchoring can be controlled, certain external mechanical excitations can be recognized and transmitted to the central nervous system, and the outer hair can be kept in relative movement via respective nerves. There are two modes the vibrissa can work in: in the *passive mode* the vibrissa is kept mainly at rest and the effects (like bending or fluttering) of external perturbations are recognized, whereas in the *active mode* the vibrissa is kept in permanent vibration in order to scan the environment.

It is obvious that *artificial vibrissae* could play an important role in robotics. To this end mathematical descriptions of properties and behavior

of vibrissae are inevitable. They must be based on results out of biological fields which in the first instance suggest appropriate physical models leading to corresponding mathematical framework. Plenty of papers on this topic can be found in literature, we just quote some local theses: The 2008 (biologically flavored) doctoral thesis by Kathrin Carl [2], the 2011 master thesis by Tonia A.Schmitz [3], and the (still unpublished) habilitation thesis by Carsten Behn [1], they all present also a lot of references. The mechanical models proposed therein are for the most part rigid body systems of degree of freedom one, two, or three (multiple pendulums with compliant support) to be evaluated by means of, e.g., Lagrange's equations. As far as theory is in the foreground, investigations of continuum models (flexible rods) are concentrated to small amplitude vibrations and treated within a linear theory, see also the 1998 paper by Ueno et al. [6]. Somewhat deviating in the way of treatment is the 2004 paper by Scholz and Rahn [4] about profile sensing by means of vibrissa sweep past an object. Here the authors exploit an experimental set-up and enter the measured data into the (non-linear) to-be-integrated bending rod equations. In 2010, Solomon and Hartmann revisit this sweep method in an improved way [5].

In the following we envisage a *vibrissa in passive mode* which is to scan an external obstacle. Opposite to [4] this is not done by sweep but while passing by. The rod is modeled as an elastical Euler-Bernoulli bending rod, the process is confined to $\mathbb{R}^2$ and runs slow (quasistatically), the profile of the obstacle is assumed to be smooth and convex. Aim is at a far-reaching analytical treatment, attempting to characterize certain process marks (like the final 'snap off'). Evaluation by computer (using Maple 15) is put to the end and this then yields a sketch of the process and the course of the observables.

Just for the sake of comparison the same problem is tackled with the help of the simplest rigid body model.

The conclusion offers some problems to be tackled in near future. An Appendix gives some hints to elliptic integrals.

2 The continuum model

We shall consider the vibrissa as an elastic rod of length L and of constant bending stiffness EI_z . Let its original unperturbed position be vertical with clamped lower end and free upper end. Let the lower end move along a horizontal straight line, whereby the upper flexible part eventually contacts an obstacle. Passing the obstacle slow, a quasistatic deformation of the rod occurs which induces certain reactions in the clamp (where the real vibrissa

ends in the follicle-sine-complex). These reactions can be observed and are hoped to admit some conclusions about the shape of the obstacle.

In order to do all calculations in a form as clear as possible we introduce once for all the following *units of measure*:

$$[length] = L\ ;\ \ [force] = EI_z L^{-2}\ ;\ \ [moment] = EI_z L^{-1}\ .$$

These units are conform to the general problem, make all formulas free of ballast (e.g., the vibrissa now has formal length 1), and the formulas match any special problem of what dimension ever.

Supposition:

Let the profile of the obstacle be a smooth strictly convex schlicht curve over the $x-$axis (where the vibrissa clamp at low speed moves in negative direction) with maximum distance > 1 and minimum distance $p_0 \in (0,1)$. Due to strict convexity the profile curve can be given in a parametrization by its slope $\alpha \in (-\frac{\pi}{2}, \frac{\pi}{2})$

$$\begin{array}{l} x = \xi(\alpha),\ \ y = \eta(\alpha),\ \ \xi(0) = 0,\ \eta(0) = p_0,\ \text{curvature } \kappa_p > 0, \\ \text{arc length}:\ \ \sigma = \int_0^\alpha [\xi'(\alpha)^2 + \eta'(\alpha)^2]^{1/2} d\alpha, \end{array}$$

with respect to a fixed (x,y)-coordinate system.

As an example take a parabola: $\xi = \tan(\alpha),\ \ \eta = p_0 + \frac{1}{2}\tan^2(\alpha)$.

For the vibrissa in passing that obstacle from the right to the left one should expect a scenario like this: A preceding phase 0 without contact is followed by a phase 1 of tangent touch with the contact point first going down the vibrissa and then again up to the vibrissa tip. During a phase 2 the vibrissa tip touches the profile under a non-zero angle until this angle equals $\frac{\pi}{2}$, then the vibrissa snaps back to the vertical position.

The analysis quickly shows that the phase 2 as described above is not correct, it terminates earlier.

Anyway, we start with an investigation of the elastica in contact with the obstacle under the

Supposition: The contact vibrissa - obstacle is ideal, i.e., the corresponding contact force is normal to the profile (no friction).

We represent the elastica as a curve in the $(x,y)-$plane, parameterized by its arc-length, $s \in [0,1]$, foot at $s = 0$. The following investigations are based on the

Working Hypothesis WH1: The elastica is nowhere left-handed.

Hence we have the normal description

$$x' = \cos(\varphi), \quad y' = \sin(\varphi), \quad \varphi' = \kappa \leq 0, \quad s \in (0,1),$$

where φ is the slope, and the curvature κ is determined by the actual bending moment. The latter is caused by a force acting upon the vibrissa at the contact point (reaction force to contact), say at $s_1 \in (0,1]$, in the opposite direction of the normal to the profile. In phase 1 the contact is mainly at some $s_1 < 1$ and the bending moment equals zero for $s \in [s_1, 1]$, whereas in phase 2 contact is at $s_1 = 1$ throughout.

2.1 Phase 1

Phase 1 starts at the very first contact of the vertical vibrissa with the profile. This is at the profile point $(\xi(\alpha_{0r}), \eta(\alpha_{0r}))$ with $\eta(\alpha_{0r}) = 1$, $\alpha_{0r} \in (0, \frac{\pi}{2})$. Let $\alpha < \alpha_{0r}$ be any *given* touch point, then the contact force is $\mathbf{f} = f \cdot (\sin(\alpha)\mathbf{e}_x - \cos(\alpha)\mathbf{e}_y)$ with unknown $f > 0$, and it acts upon the vibrissa at an unknown point s_1. The bending moment is

$$m(s,\alpha) = \begin{cases} f\{[y(s) - \eta(\alpha)]\sin(\alpha) + [x(s) - \xi(\alpha)]\cos(\alpha)\} < 0, & s \in [0, s_1), \\ 0, \quad s \in (s_1, 1]. \end{cases} \tag{1}$$

The natural bending equation then is $\kappa = m$.[1] It is more convenient to increase the order of the differential equation, coming up with the splitting boundary value problem on $(0, s_1)$

$$\begin{array}{llll} 1) & x' = \cos\varphi\,, & & (a1) \quad x(s_1) = \xi(\alpha), \\ 2) & y' = \sin\varphi\,, & (b) \quad y(0) = 0\,, & (b1) \quad y(s_1) = \eta(\alpha), \\ 3) & \varphi' = \kappa\,, & (c) \quad \varphi(0) = \frac{\pi}{2}\,, & (c1) \quad \varphi(s_1) = \alpha\,, \\ 4) & \kappa' = f\cos(\varphi - \alpha)\,, & & (d1) \quad \kappa(s_1) = 0\,. \end{array} \tag{2}$$

The boundary value problem shows up with two unknown parameters, f and s_1 (remind that α is considered prescribed).

The position of the vibrissa's clamp is at $x_0 = x(0)$ which follows from the solution of the boundary value problem. We do not need to consider the moment-free part of the vibrissa since it appears just as a straight line smoothly prolonging the first part.

The advantage of this 4th order formulation is obvious: the subproblem (3,4,c1,d1) admits a *first integral*,

$$\kappa^2 = 2f\sin(\varphi - \alpha),$$

[1] Holds for phase 2, too. Hence a sketch shows that this equation together with WH1 excludes the configuration expected above to end phase 2.

which serves as the basis for tackling the remaining equations.

As κ is negative, $\varphi(s)$ runs monotonically from $\frac{\pi}{2}$ down to α, hence $\varphi-\alpha \in (0,\pi)$, and therefore

$$\kappa = \varphi' = -\sqrt{2f}\sqrt{\sin(\varphi-\alpha)} \tag{3}$$

We observe that the reaction moment of the clamp follows with $\varphi(0)=\frac{\pi}{2}$ as

$$m_0 = \sqrt{2f\cos(\alpha)}.$$

Regarding the boundary condition (c), separation of variables in (3) yields the *2nd integral* by means of the elliptic integral $\mathbb{F}$ (see Appendix). For the sake of brevity in the sequel we introduce the auxiliary function

$$\mathbb{H}_1 : x \mapsto \mathbb{H}_1(x) := \mathbb{F}(\sqrt{2}\sin(\frac{\pi}{4}-\frac{x}{2}), \frac{1}{\sqrt{2}}), \tag{4}$$

and we put

$$h(\alpha) := \mathbb{H}_1(\frac{\pi}{2}-\alpha) = \mathbb{F}(\sqrt{2}\sin(\frac{\alpha}{2}), \frac{1}{\sqrt{2}}) \ .$$

There holds $\mathbb{H}_1(0) = h(\frac{\pi}{2}) = \mathbb{K}(\frac{1}{\sqrt{2}}) \approx 1.854$. The 2nd integral then writes

$$\boxed{\sqrt{f}\cdot s = \mathbb{H}_1(\varphi-\alpha) - h(\alpha).} \tag{5}$$

Since $\mathbb{H}_1$ is monotonic this equation solves for φ,

$$\varphi = \alpha + \mathbb{H}_1^{-1}(\sqrt{f}s + h(\alpha)). \tag{6}$$

This describes the slope of the elastica completely [2] as soon as we know f. But no more than

$$\sqrt{f}s_1 = h(\frac{\pi}{2}) - h(\alpha) \tag{7}$$

follows from (5). Clearly, to get knowledge of s_1, i.e., about *where* the contact point is located on the vibrissa, the solution $(x(\cdot), y(\cdot))$ of the first two differential equations in (2) has to be considered.

Using (6) this solution follows by quadrature

$$\begin{aligned} x(s) &= x_0 + \textstyle\int_0^s \cos(\alpha + \mathbb{H}_1^{-1}(\sqrt{f}t + h(\alpha))dt, \\ y(s) &= \textstyle\int_0^s \sin(\alpha + \mathbb{H}_1^{-1}(\sqrt{f}t + h(\alpha))dt, \end{aligned}$$

[2] For evaluations it is recommended to give $\mathbb{H}_1^{-1}$ a polynomial approximation of low degree, say, equal to 4.

or, equivalently

$$\boxed{\begin{array}{l} x(s) = x_0 + \frac{1}{\sqrt{f}} \int_{h(\alpha)}^{\sqrt{f}s+h(\alpha)} \cos(\alpha + \mathbb{H}_1^{-1}(\tau))d\tau, \\ \\ y(s) = \frac{1}{\sqrt{f}} \int_{h(\alpha)}^{\sqrt{f}s+h(\alpha)} \sin(\alpha + \mathbb{H}_1^{-1}(\tau))d\tau. \end{array}} \tag{8}$$

Putting $s = s_1$ and again using (7) we obtain from the remaining boundary conditions

$$y(s_1) = \frac{1}{\sqrt{f}} \int_{h(\alpha)}^{h(\frac{\pi}{2})} \sin(\alpha + \mathbb{H}_1^{-1}(\tau))d\tau = \eta(\alpha), \tag{9}$$

which is an equation for f in configuration α,

$$f(\alpha) = [\frac{1}{\eta(\alpha)} \int_{h(\alpha)}^{h(\frac{\pi}{2})} \sin(\alpha + \mathbb{H}_1^{-1}(\tau))d\tau]^2, \tag{10}$$

and then

$$x(s_1) = x_0 + \frac{1}{\sqrt{f(\alpha)}} \int_{h(\alpha)}^{h(\frac{\pi}{2})} \cos(\alpha + \mathbb{H}_1^{-1}(\tau))d\tau = \xi(\alpha), \tag{11}$$

which now gives $x_0(\alpha)$. Finally, s_1 follows from (7),

$$s_1(\alpha) = \eta(\alpha)\{h(\frac{\pi}{2}) - h(\alpha)\}[\int_{h(\alpha)}^{h(\frac{\pi}{2})} \sin(\alpha + \mathbb{H}_1^{-1}(\tau))d\tau]^{-1}. \tag{12}$$

The open domain of phase 1 is $\{\alpha : s_1(\alpha) < 1\}$. While (physically) the foot coordinate x_0 monotonically displaces from $\xi(\alpha_{0r}) > 0$ to the left, α decreases monotonically, and the simultaneous ride of the touch point s_1 on the elastica is $1 \searrow s_{11} < 1 \nearrow 1$. Hence phase 1 terminates at $\alpha_1 = \inf\{\alpha \in (\alpha_{0l}, \alpha_{0r}) \mid s_1(\alpha) < 1\}$[3]. This parameter $\alpha =: \alpha_1$ that terminates phase 1 is now a solution of the equation

$$\int_{h(\alpha)}^{h(\frac{\pi}{2})} \sin(\alpha + \mathbb{H}_1^{-1}(\tau))d\tau = \eta(\alpha)\{h(\frac{\pi}{2}) - h(\alpha)\}, \tag{13}$$

which follows from (12) with $s_1 \to 1$.

It is easy to calculate that $\alpha_1 = 0$ (mind $\eta(0) = p_0$) iff

$$p_0 = \underline{p_0} := .4569465811$$

[3] $\alpha_{0l} < 0$ characterizes the utmost left possible touch point, $\eta(\alpha_{0l}) = 1$.

whereas $\alpha_1 \gtreqless 0$ if $p_0 \gtreqless \underline{p_0}$.

The contact force given by (10), is, so far, that one (of slope $\frac{\pi}{2} - \alpha$) which brings the point of its action upon the elastica to the altitude $\eta(\alpha)$ with local slope $\varphi = \alpha$ of the elastica. The foot coordinate x_0 given by (11) then ensures that this point is at $(\xi(\alpha), \eta(\alpha))$ on the obstacle (now *touch* point). Finally, the location of that point on the elastica is given by (12).

2.2 Phase 2

During this phase the vibrissa tip contacts the profile at some point $(\xi(\alpha), \eta(\alpha))$ with $\alpha < \alpha_1$, with vibrissa (end-)slope $\varphi(1) =: \varphi_1 > \alpha$. The contact force is again normal to the profile, so the bending moment is

$$m(s, \alpha) = f\{[y(s) - \eta(\alpha)]\sin(\alpha) + [x(s) - \xi(\alpha)]\cos(\alpha)\}, \quad s \in [0, 1].$$

The boundary value problem now is

$$\boxed{\begin{array}{llll} 1) & x' = \cos\varphi\ , & & (a1) \quad x(1) = \xi(\alpha), \\ 2) & y' = \sin\varphi\ , & (b) \quad y(0) = 0\ , & (b1) \quad y(1) = \eta(\alpha), \\ 3) & \varphi' = \kappa\ , & (c) \quad \varphi(0) = \frac{\pi}{2}\ , & \\ 4) & \kappa' = f\cos(\varphi - \alpha)\ , & & (d1) \quad \kappa(1) = 0\ . \end{array}} \tag{14}$$

Again, the subproblem (3,4,d1) has a *first integral* which, taking into account $\varphi(1) = \varphi_1$ with still unknown $\varphi_1 > \alpha$, now reads

$$\kappa^2 = 2f[\sin(\varphi - \alpha) - \sin(\varphi_1 - \alpha)]. \tag{15}$$

About domains:

In phase 2 we have $-\frac{\pi}{2} < \alpha_{0l} < \alpha < \alpha_1, \ \ \alpha < \varphi_1 \le \varphi \le \frac{\pi}{2}$. Hence (15) is with

$$0 \le \varphi_1 - \alpha \le \varphi - \alpha \le \frac{\pi}{2} - \alpha \ \begin{cases} \le \frac{\pi}{2} - \alpha_{0l} \le \pi, \text{ if } \alpha < 0 \\ \le \frac{\pi}{2}, \text{ if } \alpha \ge 0 \end{cases}.$$

Further restrictions arise from the demand $\kappa^2 \ge 0$ for all $\varphi \in [\varphi_1, \frac{\pi}{2})$. To find these out we rewrite (15)

$$\kappa^2 = 4f \cdot \sin(\frac{\varphi - \varphi_1}{2}) \cdot \cos(\frac{\varphi + \varphi_1 - 2\alpha}{2}).$$

a) Both trigonometric factors ≤ 0: already the first one demands

$$-2\pi \le \varphi - \varphi_1 \le 0 \quad \vee \quad 2\pi \le \varphi - \varphi_1 \le 4\pi$$

which contradicts the inequalities above.
b) Both trigonometric factors ≥ 0: then

$$0 \leq \varphi - \varphi_1 \leq 2\pi \quad \wedge \quad -\pi \leq \varphi + \varphi_1 - 2\alpha \leq \pi,$$

together with the restrictions at the beginning entail

$$\alpha < \varphi_1 \leq \min\{\frac{\pi}{2}, \frac{\pi}{2} + 2\alpha\} = \begin{cases} \frac{\pi}{2} + 2\alpha, \ if \ \alpha < 0, \\ \frac{\pi}{2}, \ if \ \alpha \geq 0, \end{cases} \tag{16}$$

or, equivalently,

$$0 < \varphi_1 - \alpha \leq \frac{\pi}{2} - \mid \alpha \mid . \tag{17}$$

Obeying these restrictions of φ_1 we get the curvature of the elastica from (15) in the form

$$\kappa(\varphi, \varphi_1, \alpha) = -\sqrt{2f}[\sin(\varphi - \alpha) - \sin(\varphi_1 - \alpha)]^{1/2}, \tag{18}$$

with f certainly depending on φ_1 and α.

Now separation of variables in the initial value problem $\varphi' = \kappa, \ \varphi(0) = \frac{\pi}{2}$ yields the second integral [4]

$$\boxed{\begin{array}{l} \sqrt{f} \cdot s = \mathbb{F}(\frac{1}{k}\sin(\frac{\pi}{4} - \frac{1}{2}(\varphi - \alpha)), k) - \mathbb{F}(\frac{1}{k}\sin(\frac{\alpha}{2}), k), \\ with \ \ k = \sin(\frac{\pi}{4} - \frac{1}{2}(\varphi_1 - \alpha)). \end{array}} \tag{19}$$

For brevity and following the lines in Section 1.1 we introduce the function

$$\mathbb{H}_2 : (x, u) \mapsto \mathbb{F}(\frac{\sin(\frac{\pi}{4} - \frac{x}{2})}{\sin(\frac{\pi}{4} - \frac{u}{2})}, \sin(\frac{\pi}{4} - \frac{u}{2}))$$

for $0 \leq u \leq x \leq \frac{\pi}{2} - \alpha$. Then (19) writes

$$\sqrt{f} \cdot s = \mathbb{H}_2(\varphi - \alpha, \varphi_1 - \alpha) - \mathbb{H}_2(\frac{\pi}{2} - \alpha, \varphi_1 - \alpha). \tag{20}$$

At $s = 1, \ \varphi(1) = \varphi_1$ we get an expression for the contact force f,

$$\sqrt{f(\varphi_1, \alpha)} = \mathbb{H}_2(\varphi_1 - \alpha, \varphi_1 - \alpha) - \mathbb{H}_2(\frac{\pi}{2} - \alpha, \varphi_1 - \alpha). \tag{21}$$

Remark 1 *Mind that the close relation of phases 1 and 2 shows up by the identity* $\mathbb{H}_1(x) = \mathbb{H}_2(x, 0)$*; compare (5) and (19). While in phase 1 the touch point coordinate* s_1 *on the elastica was unknown and the touch angle* $\varphi_1 = \alpha$ *was given, we have now* $s_1 = 1$ *given whereas* φ_1 *appears as unknown.*

[4] $0 \leq \mid \alpha \mid /2 \leq \frac{1}{2}(\frac{\pi}{2} - (\varphi_1 - \alpha)) < \frac{\pi}{4}$ by(17), implies $k > 0$.

In regard of the second argument of $\mathbb{H}_2$ it is not recommendable to proceed on the first way used in Section 1.1. That is since the inverse $(\mathbb{H}_2(\cdot,u))^{-1}$ would now appear as a *family* of functions.

So let us turn to a different way of treatment (which could have been followed in Section 1.1, too). Rewrite the upper two lines in (14) in the respective form for $\varphi \mapsto (x,y)(\varphi)$ with κ taken from (18) and f from (21),

$$\begin{aligned} \frac{dx}{d\varphi} &= \frac{1}{\kappa(\varphi,\varphi_1,\alpha)}\cos(\varphi), \quad x(\varphi_1)=\xi(\alpha), \\ \frac{dy}{d\varphi} &= \frac{1}{\kappa(\varphi,\varphi_1,\alpha)}\sin(\varphi), \quad y(\varphi_1)=\eta(\alpha), \quad y(\frac{\pi}{2})=0. \end{aligned}$$

As a first step, we solve the y initial value problem ignoring the first boundary condition while letting φ_1 and α as parameters,

$$y(\varphi,\varphi_1,\alpha) = -\frac{1}{\sqrt{2f(\varphi_1,\alpha)}}\int_{\pi/2}^{\varphi}\sin(t)[\sin(t-\alpha)-\sin(\varphi_1-\alpha)]^{-1/2}dt.$$

By (21) f is known as dependent on φ_1 and α. In order to find the correct φ_1 belonging to α, we exploit the condition $y(\varphi_1)=\eta(\alpha)$ as an equation for $\varphi_1=\varphi_1(\alpha)$:

$$-\int_{\pi/2}^{\varphi_1}\sin(t)[\sin(t-\alpha)-\sin(\varphi_1-\alpha)]^{-1/2}dt = \eta(\alpha)\sqrt{2f(\varphi_1,\alpha)}. \qquad (22)$$

Putting $y(\varphi,\varphi_1(\alpha),\alpha) =: y(\varphi,\alpha)$ and $f(\alpha) := f(\varphi_1(\alpha),\alpha)$ the elastica is now described as

$$\boxed{\begin{array}{l} x(\varphi,\alpha) = \xi(\alpha) - \frac{1}{\sqrt{2f(\alpha)}}\int_{\varphi_1(\alpha)}^{\varphi}\cos(t)[\sin(t-\alpha)-\sin(\varphi_1(\alpha)-\alpha)]^{-1/2}dt, \\ \\ y(\varphi,\alpha) = -\frac{1}{\sqrt{2f(\alpha)}}\int_{\pi/2}^{\varphi}\sin(t)[\sin(t-\alpha)-\sin(\varphi_1(\alpha)-\alpha)]^{-1/2}dt. \end{array}} \qquad (23)$$

The vibrissa's foot is at $x_0(\alpha) = x(\frac{\pi}{2},\alpha)$.

The **observables** (clamp reactions) are

$$-\mathbf{f}(\alpha) \text{ and } m_0(\alpha) = \kappa(\frac{\pi}{2},\varphi_1(\alpha),\alpha) = -\sqrt{2f(\alpha)}[\cos(\alpha)-\sin(\varphi_1(\alpha)-\alpha)]^{1/2}.$$

Mind that for $\varphi_1=\alpha$ (characterizing phase 1) these expressions coincide with the respective ones from Section 2.1.

Still to be cleared at the very end: *Which $\alpha=\alpha_2$ terminates phase 2 ?* We sketch three seemingly reasonable scenarios for terminating phase 2.

(a) Phase 2 terminates at the first contact point that makes the reaction moment at the vibrissa foot vanish. This means that the contact force $\mathbf{f}$ aims at the foot.
Criticism: The zero moment in both the clamp and the contact point shows the configuration like one of buckling between two pivots. Then $\varphi \mid_{s=0} = \frac{\pi}{2}$ entails $\varphi_1 = 0$ due to symmetry. On the other hand we see from the observables formula above that m_0 vanishes at $\alpha = -\frac{\pi}{4}$ if $\varphi_1 = 0$. Furthermore it must hold $(\xi(\alpha) - x_0(\alpha))^2 + \eta(\alpha)^2 = L^2$, where L is the distance of the supports of a buckling rod with boundary slope $\alpha = \alpha_2$. And this had to be true for every profile! *This scenario turns out to be dubious!*

(b) Phase 2 ends at an α_2 s.t. for $\alpha < \alpha_2$ a negative f is needed to ensure contact (*pulling* the vibrissa tip). For the sake of continuity this entails $f(\alpha_2) = 0$.
Criticism: The complete (last contact) configuration at α_2 is then governed by $f = 0$, i.e., $\kappa = 0$ and $\varphi = \frac{\pi}{2}$ for all $s \in [0, 1]$, and this would imply $\alpha_2 = \alpha_{0l}$ (no "early" end of phase 2).

(c) Wellknown from (21) and (22): for each $\alpha \in (\alpha_{0l}, \alpha_1]$ there is a force $f(\alpha)$ of slope $\alpha - \frac{\pi}{2}$ s.t. $y \mid_{s=1} = \eta(\alpha)$. Then there exists a unique $x_0(\alpha)$ ensuring $x \mid_{s=1} = \xi(\alpha)$.
Now remind that (physically) the primary "drive" is a motion of the vibrissa's foot monotonically to the left. Starting each step in calculation with a prescribed α (instead of a foot coordinate) is only a trick to simplify things to do!
So, if the function $x_0(\cdot)$ - which is calculated pointwise on a decreasing $\alpha-$sequence - shows a local minimum at some α_2, then the physical process $x_0 \Downarrow$ breaks down and α_2 terminates phase 2.

Most likely, this last α_2 is the correct one, its determination needs a procedure as follows.
For each α running along a sufficiently dense sequence ($\alpha_{(i)} = \alpha_1 + i \cdot \delta\alpha,\ \delta\alpha < 0$) do this chain of calculations:
1) from (21) take the function $f(\varphi_1, \alpha)$;
2) consider the equation (22) for $\varphi_1 = \varphi_1(\alpha)$; there are two options (to be verified by computing):
a) with $\alpha = \alpha_{(i)}$ the equation has no solution $\varphi_1(\alpha) \in (\alpha, \frac{\pi}{2} - \alpha^-)$, i.e., at $\alpha_{(i)}$ no equilibrium configuration exists: α_2 has been passed, phase 2 has ended;
b) there is a solution $\varphi_1(\alpha)$, i.e., under the force $f(\alpha) := f(\varphi_1(\alpha), \alpha)$ the tip of the elastica is at height $\eta(\alpha)$; then
3) find $x_0(\alpha) = x(\frac{\pi}{2}, \alpha)$ from (23) and check whether this current $x_0(\alpha_{(i)}) < 0$ is smaller than $x_0(\alpha_{(i-1)})$, if not, then α_2 has been passed and the process must be stopped.

This item deserves further more detailed consideration.

2.3 Examples

In the following two worked examples are presented: scanning a catenary profile and an asymmetric profile composed of two circles. The figures show the configurations and the behavior of some observables.

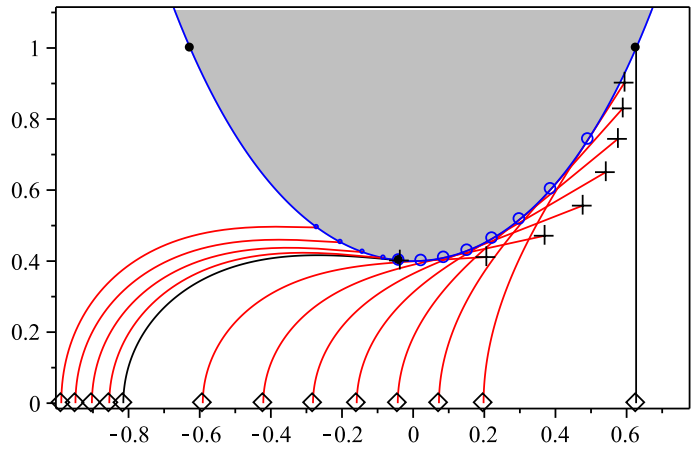

Figure 2.1: Scanning a catenary

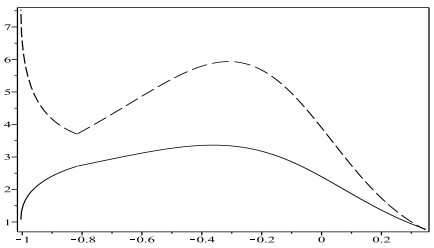

Figure 2.2: Observables m_0 (solid) and f (dash) vs. foot coordinate x_0

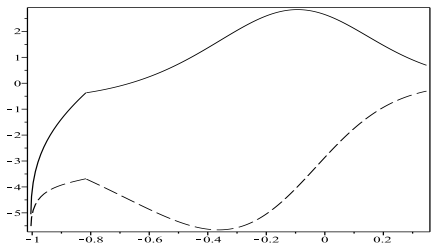

Figure 2.3: Observables f_x (solid) and f_y (dash) vs. foot coordinate x_0

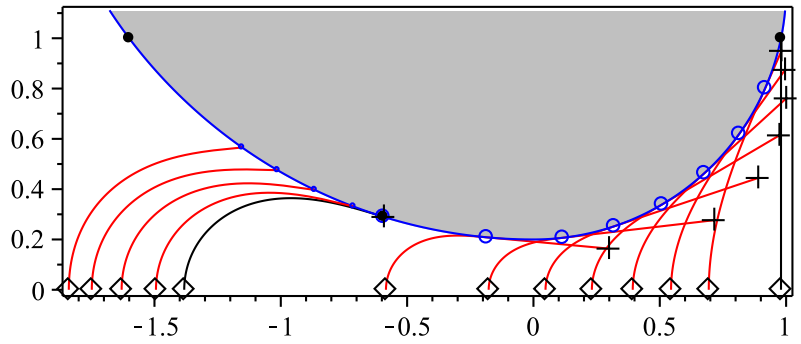

Figure 2.4: Scanning a profile composed of two circles

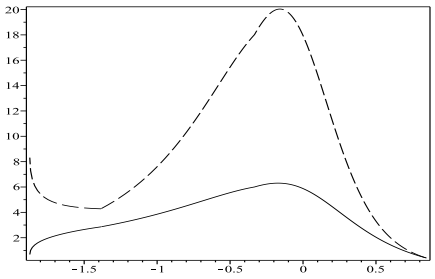

Figure 2.5: Observables m_0 (solid) and f (dash) vs. foot coordinate x_0

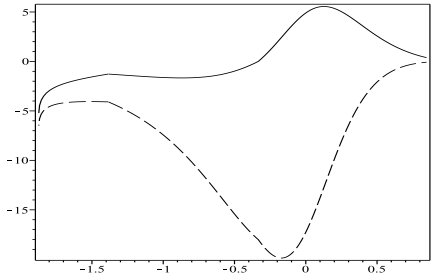

Figure 2.6: Observables f_x (solid) and f_y (dash) vs. foot coordinate x_0

3 About discrete models

It is natural that a flexible thin rod is the appropriate model of a vibrissa. Nevertheless, models of finite degree of freedom found their place in the theses [1] and [3] and in foregoing more biologically flavored papers as well. Principally, they are controlled multiple pendulum systems with visco-elastic

joints and support. In the following we give a sketch of the simplest one of these models, appearing as a pendulum of degree of freedom equal to 1, which serves for quasistatically scanning an obstacle as in the preceding section.

Now we consider the vibrissa as a rigid rod of length L in an $(x, y)-$plane with original unperturbed vertical position. Let its lower end be elastically pivoted to the $x-$axis and moving slow along it. Eventually, the rod may be in ideal contact with an obstacle as described in Section 2. Let c be the stiffness of the elastical pivot. Then we use here the following *units of measure*:

$$[length] = L; \;\; [moment] = c; \;\; [force] = cL^{-1}.$$

As done before we introduce the arc-length $s \in [0, 1]$ along the rod, ($s = 0$: lower end). If the lower pivoted end is placed at x_0, then it is pure geometry to describe the configuration of the rod being in contact with the obstacle. There are again two modes of configuration:
Mode 1: tangential touch at $s_1 \leq 1$ with the profile at α, angle of inclination of the rod equals $\varphi = \alpha$;
Mode 2: non-tangential touch at $s_1 = 1$ with the profile at α, angle of inclination of the rod is $\varphi > \alpha$.

In both cases a reaction force $\mathbf{f}_0$ and a moment $m_0 = \frac{\pi}{2} - \varphi$ at $s = 0$ and a reaction force $\mathbf{f}$ at $s = s_1$ act upon the rod in equilibrium; under ideal contact the force $\mathbf{f}$ is in outer normal direction to the profile. The general geometry is simply

$$s_1 \sin(\varphi) = \eta(\alpha), \;\; s_1 \cos(\varphi) = \xi(\alpha) - x_0(\alpha),$$

and the statics comprises in

$$m_0 - f s_1 \cos(\varphi - \alpha) = 0 \;\; , \;\; f \geq 0; \;\; \mathbf{f} + \mathbf{f}_0 = 0.$$

So, mode 1 is characterized by $\sin(\alpha) > \eta(\alpha)$ (implies $\alpha > 0$, and its domain is bounded by α_1 and $\alpha_2 : \eta(\alpha) = \sin(\alpha)$) with $f(\alpha) = (\frac{\pi}{2} - \varphi)\sin(\alpha)/\eta(\alpha)$. Mode 2 is characterized by $\sin(\alpha) < \eta(\alpha)$, $\tan(\varphi) = \eta(\alpha)/\sqrt{1 - \eta(\alpha)^2}$ and

$$f(\alpha) = (\frac{\pi}{2} - \varphi)[\sqrt{1 - \eta(\alpha)^2}\cos(\alpha) + \eta(\alpha)\sin(\alpha)]^{-1}.$$

The scanning process begins at $x_0 = \xi(\alpha_0), \; \eta(\alpha_0) = 1, \; \alpha_0 > 0$ at time $t = 0$, say, and proceeds in accordance with $x_0 = \xi(\alpha_0) - v_0 t$ ($v_0 > 0$ small velocity). Start is in mode 1 if $\alpha_0 = \frac{\pi}{2}$ or in mode 2 if $\alpha_0 < \frac{\pi}{2}$. The process ultimately terminates and is followed by a 'snap back' when the rod is orthogonal to the profile, i.e., for

$$\varphi = \alpha + \frac{\pi}{2}, \; \cos(\alpha) = \eta(\alpha)$$

(yields $f(\alpha) = +\infty$, which has a flair of irreality, maybe this is caused by the absence of friction, i.e., omitting any profile roughness from the model; anyway, it is a hint to the inadequacy of this model).

3.1 Example

As an example we present the scanning of an obstacle with parabolic profile:

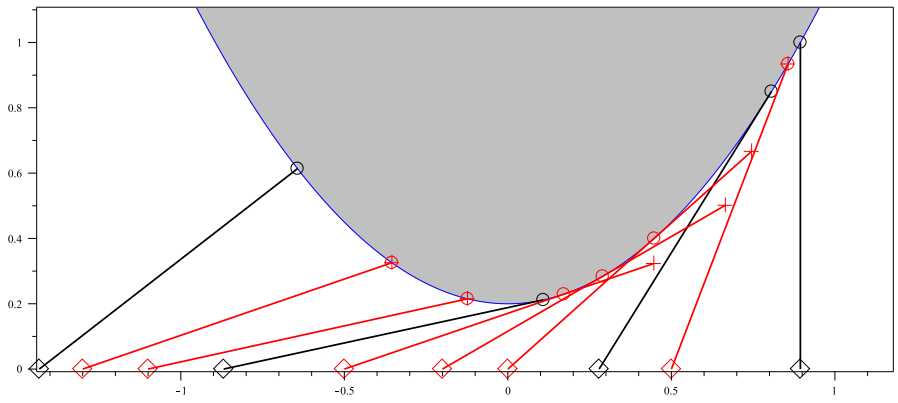

Figure 3.1: Scanning a parabola.

Besides **f** the main obervable might be the moment m_0 in dependence on the foot coordinate x_0. Moreover, also the contact coordinate on the rod, s_1, could be observed if the rod was endowed with a series of sensors:

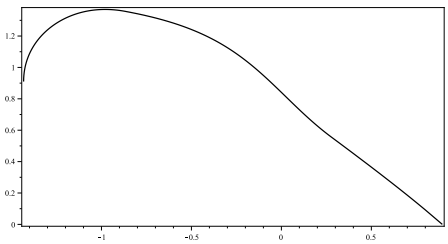

Figure 3.2: : m_0 vs. x_0

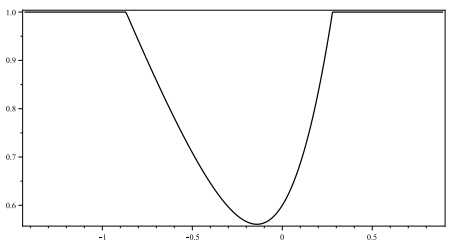

Figure 3.3: : s_1 vs. x_0

4 Conclusion

The foregoing investigations are to be understood as a starting-point of further advances in the theory of (artificial) vibrissae. We sketch some urgent tasks for improvement.

For a better approach to real vibrissae the basic differential equations should be expanded to cover rods with non-constant bending stiffness (hollow conical rod) and a pre-curvature. The corresponding ODEs may then demand a purely numerical treatment and a specially tailored software. Another access should be to model the vibrissa by means of super-elements from multi-body dynamics and to utilize corresponding software like ALASKA.

Any reasonable implementation and application need an answer to the question *'how to infer the shape of the scanned profile from the determined function* $x_0 \mapsto$ *observables'*.

In order to scan a 3-dimensional obstacle a 2-dimensional field of vibrissae is necessary. The vibrissae have to be modeled as rods which deform in $\mathbb{R}^3$. The outputs of all vibrissae of the field have to undergo a simultaneous coupled analysis and comparison.

Some experiments and measures with a simple set-up should be done in order to validate the theoretical results.

References

[1] Behn,C.: Mathematical Modeling and Control of Biologically Inspired Uncertain Motion Systems with Adaptive Features; *Habilitation Thesis, Ilmenau University of Technology, Faculty of Mechanical Engineering, 2013 (to be published).*

[2] Carl,K.: Technische Biologie des Tasthaar-Sinnessystems als Gestaltungsgrundlage für taktile stiftführende Mechanosensoren; *Dissertation, Ilmenau University of Technology, Faculty of Mechanical Engineering, 2008.*

[3] Schmitz,T.A.: Entwurf und Analyse von biologisch inspirierten Sensorsystemen mit erhöhtem Freiheitsgrad am Beispiel Vibrisse; *Master Thesis, Ilmenau University of Technology, Faculty of Mechanical Engineering, 2011.*

[4] Scholz,G.R., C.D.Rahn : Profile Sensing With an Actuated Whisker; *IEEE Trans. of Robotics and Autom., vol.20, no.1, 124-127, 2004.*

[5] Solomon,J.H., M.J.Z.Hartmann : Extracting Object Contours with the Sweep of a Whisker Using Torque Information; *Int. J. Robotic Research,vol.29, no.9, 1233-1244, 2010.*

[6] Ueno,N. et al.: Dynamic Contact Sensing by Flexible Beam; *IEEE/ASME Trans. Mechatronics, vol.3, no.4, 254-264, 1998.*

Appendix

Elliptic integral of 1st kind:

$$\mathbb{F}(z,k) := \int_0^z \frac{1}{\sqrt{1-t^2}\sqrt{1-k^2t^2}}dt,\ (k<1).$$

Complete elliptic integral of 1st kind:

$$\mathbb{K}(k) := \mathbb{F}(1,k).$$

Elliptic integral of 2nd kind:

$$\mathbb{E}(z,k) := \int_0^z \sqrt{\frac{1-k^2t^2}{1-t^2}}dt,\ (k<1).$$

By experience, within Maple procedures it is sometimes recommendable to rewrite integrals in a representation using these standard elliptic integrals. An example (occurring in solving (3)):

$$\boxed{I(x) := \int^x \frac{dt}{\sqrt{\sin(t)}}} = \int^x \frac{dt}{\sqrt{\cos(\frac{\pi}{2}-t)}} = -\int^{\frac{\pi}{2}-x} \frac{du}{\sqrt{\cos(u)}}\ ;$$

$$z := \sqrt{2}\sin(\tfrac{u}{2}),\ \ dz = \tfrac{1}{\sqrt{2}}\sqrt{1-\tfrac{1}{2}z^2}du,\ \ \cos(u) = 1-z^2\ ;$$

$$\Longrightarrow\ I(x) = -\sqrt{2}\int^{\sqrt{2}\sin(\frac{\pi}{4}-\frac{x}{2})}[(1-z^2)(1-\tfrac{1}{2}z^2)]^{-1/2}dz$$

$$\boxed{I(x) = -\sqrt{2}\mathbb{F}(\sqrt{2}\sin(\tfrac{\pi}{4}-\tfrac{x}{2}),\tfrac{1}{\sqrt{2}}) + const.}$$